Published in final edited form as:
J Med Chem. 2010 February 25; 53(4): 1579–1586. doi:10.1021/jm901228u.

Two-step Synthesis of Galactosylated Human Serum Albumin as a Targeted Optical Imaging Agent for Peritoneal Carcinomatosis

Celeste Aida S. Regino[§], **Mikako Ogawa**[§], **Raphael Alford**[§,δ], **Karen J. Wong**[§], **Noboyuki Kosaka**[§], **Mark Williams**[§,¥], **Brain J. Field**[‡], **Masatoshi Takahashi**[‡], **Peter L. Choyke**[§], and **Hisataka Kobayashi**[§,*]

[§]Molecular Imaging Program, Center for Cancer Research, National Cancer Institute, National Institutes of Health, 10 Center Drive, Bethesda, MD 20892-1088

[δ]Howard Hughes Medical Institute, 4000 Jones Bridge Road, Chevy Chase, MD 20815-6789

[¥]Laboratory Animal Sciences Program, SAIC-Frederick, Inc., NCI-Frederick, Frederick, MD 21702

[‡]Shimazdu Scientific Instruments, 7102 Riverwood Dr., Columbia, MD 21046

Abstract

An optical probe, RG-$(gal)_{28}$GSA, was synthesized to improve the detection of peritoneal implants by targeting the β-D-galactose receptors highly expressed on the cell surface of a wide variety of cancers arising from the ovary, pancreas, colon, and stomach. Evaluation of RG-$(gal)_{28}$GSA, RG-$(gal)_{20}$GSA, glucose-analog RG-$(glu)_{28}$GSA, and control RG-HSA, demonstrates specificity for the galactose, binding to several human adenocarcinoma cell lines, and cellular internalization. Studies using peritoneally disseminated SHIN3 xenografts in mice also confirmed a preference for galactose with the ability to detect submillimeter size lesions. Preliminary toxicity study for RG-$(gal)_{28}$GSA using Balb/c mice reveal no toxic effects up to 100x of the standard imaging dose of 1mg/kg administered either intraperitoneally or intravenously. These data indicate that RG-$(gal)_{28}$GSA can selectively target a variety of human adenocarcinoma, can improve intraoperative or endoscopic tumor detection and resection, and may have little or no toxic *in vivo* effects; hence, it may be clinically translatable.

Keywords

lectin; targeted optical agent; galactosylated human serum albumin; fluorescence imaging; toxicity; ovarian cancer

Introduction

Cancer is the second leading cause of death in the U.S. accounting for ~23% of the total deaths, and is the leading cause of death for the age group of 45-64 years old.[1] Over 1.4 million new cases and about 560,000 deaths were estimated to be caused by cancer in 2007 for the US alone.[2] A yearly estimate of about 22,000 new cases and 15,000 deaths are expected to be due to ovarian cancer in American women.[2] Due to non-specific symptoms of ovarian cancer which can cause delay in diagnosis, diagnosis in the late stage and a poor

[*]10 Center Drive Bldg 10 Rm 1B40 MSC 1088 Bethesda, MD 20892-1088 Tel No: (301) –435-4086 Fax No: (301)-402-3191 kobayash@mail.nih.gov .

Supporting Information Synthesis of the ggHSA as an alternative route to galactosylated HSA, SE-HPLC, gel electrophoresis, additional in vitro and in vivo, results for the compounds. This material is available free of charge via the Internet at http://pubs.acs.org.

prognosis, disease management involves intensive therapy to treat advanced disease. Ovarian cancer often spreads the peritoneum where it is difficult to localize and treat.

Patients suffering from peritoneal dissemination of cancer, either from primary peritoneal cancer or from peritoneal metastasis of ovarian cancer, often have a poor prognosis.Treatment includes aggressive cytoreduction followed by systemic or peritoneal chemotherapy. The extent to which the tumor can be debulked is directly related to prognosis with resections resulting in “no visible disease” providing the best outcome. However, recurrence rates are high even after removal of all visible disease implying subvisible disease remains at the time of cytoreduction. Herein, we propose to use optical fluorescence imaging to improve the detection of cancers by providing real-time imaging of the peritoneum. Cancer-specific fluorescent probes are believed to improve cancer detection in surgical resection due to their sensitivity, low cost, compatibility with the surgical environment, and the absence of ionizing radiation.

Three approaches have been used in the application of fluorescent probes for cancer detection or visualization. One technique would be to use cancer cells engineered to express fluorescence such as green fluorescent protein [3-6] illuminating only fluorescently-expressing cancer cells and keeping the background signal low. This would have the advantage of directly tracking the cancer cell and would be independent of the surface protein receptor expression a ligand would otherwise be dependent on. However, gene transfection for each type of target cancer cell line to express the fluorescent protein would be required. The second approach would be to introduce novel telomerase-dependent replication-competent adenovirus expressing the fluorescence to target the cancer cells.[7] Using this method, only the presence of highly active telomerase such as those in malignant tissue fluoresced brightly. However, replication of the virus in the cancer cell/tissue would be needed in order for the appreciable fluorescence to be detected and this can take up to 5 days post-administration.[7] Third approach used would be to conjugate a dye to a ligand that targets surface protein receptors expressed by cancer cells. The background signal may be higher due to the presence of the circulating dye-ligand conjugate and can also target other cells expressing the target receptors. Then again, this can be more widely applicable in terms of targeting a surface protein receptors that is expressed in a variety of cancer and even on one particular cancer that are heterogenous in nature composed of two or more types of cells but still have similar surface protein receptors. This approach also allows imaging after a short period of time, in this study ~4 hr, after administration of the agent.

An optical dye conjugated to a targeting moiety would be our ideal choice for a targeted optical agent. We have chosen to target the lectins (of the asialo receptor family), specifically the β-D-galactose-specific type which have been found to be expressed on the cell surface of a variety of ovarian peritoneal metastasis as well as other cancer cell lines.[8, 9] This lectin receptor binds and internalizes terminal galactosylated proteins.[10] Previous studies have demonstrated *in vitro* binding and *in vivo* targeting of lectin receptors in ovarian cancer cell lines using Rhodamine Green conjugated to avidin or to galactosylated bovine serum albumin.[9, 11-15] In these studies, submillimeter sizes of tumors have been detected in intraperitoneally disseminated xenografts of a human tumor ovarian cell line SHIN3 in mice.

Clinical translation of this lectin-targeting optical agent necessitates the use of non-immunogenic compounds. Avidin is known to cause immunogenic reactions to humans (human anti-avidin response or HAAR)[16] whereas ^{99m}Tc-DTPA-galactosylated human serum albumin is currently being used to evaluate liver functions in patients with hepatic disorders such as cirrhosis, chronic hepatitis, and to monitor liver function after transcatheter

arterial embolization and after hepatectomy for patients suffering from hepatocarcinoma.[17-23]

Herein, we demonstrate the synthesis and efficacy of Rhodamine Green-galactosylated human serum albumin as a targeted fluorescent probe for ovarian cancer lesions *in vitro* and *in vivo* using peritoneally disseminated SHIN3 xenografts in athymic mice. We also demonstrate the selectivity of the lectin receptors for galactose over glucose as the sugar moiety. Preliminary *in vivo* toxicity studies of the agent also reveals it is non-toxic even at 100x of the dose used for *in vivo* imaging.

Results

Synthesis of the glycosylated HSA

Mass spectral analyses of the glycosylated HSA indicates that direct glycosylation of human serum albumin gave ~28 galactosamine conjugated to HSA in 12 hr, ~20 galactosamine conjugated to HSA in 4 hr, and ~28 glucosamine conjugated to HSA in 12 hr at 37°C (Figure 1) indicating that ~28 sugars is the maximum we can attain under these conditions (reaction time, reaction pH and reaction temperature) out of the maximum 99 carboxylic acid residues on HSA.

Rhodamine Green (RG) dye conjugation gave about ~5-7 dyes per HSA as quantified spectrophotometrically. Although this number is high and the concern for self-quench is valid, once internalized the agent is dequenched and turns “on”.[24]

Endotoxin level was evaluated using a commercially available LAL gel clot kit. A positive response (opacification and gelation) on the gel clot tube indicates an endotoxin level equal to or exceeding the reagent’s labeled sensitivity. Negative responses were obtained for the different doses of RG-$(gal)_{28}$GSA and saline solutions indicating that the endotoxin level in the sample is below the reagent’s labeled sensitivity level (0.125 EU/mL). The U.S. Food and Drug Adminitration has established endotoxin limits of 5 EU/kg for intravenous drugs and 0.2 EU/kg for intrathecal drugs (http://www.fda.gov/downloads/BiologicsBloodVaccines/GuidanceComplianceRegulatoryInformation/Guidances/Blood/UCM080966.pdf). The calculated endotoxin level of our agent RG-$(gal)_{28}$GSA at 100x dose is then below 1.25 EU/kg and the calculated Minimum Valid Concentration (MVC) ([LAL kit sensitivity × maximum dose]/5 EU/kg) is 2.5 mg/mL.

In Vitro Analyses

Flow cytometry study was used to evaluate binding of the glycosylated HSA-Rhodamine Green conjugates to SHIN3 and to other cancer cell lines (Figure 2). The average percentage of fluorescence-gated cells for the Rhodamine Green conjugated $(gal)_{28}$GSA, $(gal)_{20}$GSA, and $(glu)_{28}$GSA were about 99.6 % and is significantly higher than the Rhodamine Green-HSA (RG-HSA, 64.7 %) (see Supplemental Information). The RG-$(gal)_{28}$GSA shows the largest log shift to the right (>2 log shift) compared to RG-$(gal)_{20}$GSA and RG-$(glu)_{28}$GSA having about the same right shift (1<log shift<3), and is significantly larger than RG-HSA (0.5< log shift <1) and the buffer control. Specificity of the RG-$(gal)_{28}$GSA to galactose-binding lectins was demonstrated using SHIN3 cells by the reduction in the log shift and in mean fluorescence intensity upon addition of excess unlabeled $(gal)_{28}$GSA (see Supplemental Information). Flow cytometry studies demonstrate that the ovarian adenocarcinoma cell lines exhibit higher expression of galactose-binding lectins as seen from their high mean fluorescence intensities (MFI) compared to the other cell lines and is about 60-fold higher than the mean fluorescence intensity obtained from the RG-HSA which ranges from 5 – 23 in the eight cell lines tested (see Supplemental Information).

Binding and internalization of RG-$(gal)_{28}$GSA was demonstrated in the microscopy studies. Higher fluorescence intensities and shorter exposure times were needed using RG-$(gal)_{28}$GSA while RG-$(gal)_{20}$GSA and RG-HSA demonstrated very low fluorescent intensities even at very long exposure times and no internalization of the fluorescent molecules (Figure 3).

In Vivo Optical Fluorescence Imaging

Mice bearing peritoneally disseminated xenografts of SHIN3 received an intraperitoneal injection of 20 μg in 300 μL 1x PBS of RG-$(gal)_{28}$GSA, RG-$(glu)_{28}$GSA, or RG-HSA and side-by-side spectral fluorescence images of the excised abdomen were obtained 4 hr after i.p injection. The optimization of the incubation time and imaging time has been studied from previous reports giving it ample time for the excess and unbound agent to clear out and give a high tumor-to-background ratio.[14]

The trend in terms of tumor-associated fluorescence intensity obtained with Rhodamine Green conjugates are as follows: RG-$(gal)_{28}$GSA > RG-$(gal)_{20}$GSA > RG-$(glu)_{28}$GSA > RG-HSA with the peritoneal background signal being low (Figure 4). Spectral fluorescence composite images of a portion of the bowel and mesentery of mice-treated with RG-$(gal)_{28}$GSA reveal submillimeter-sized tumor implants which were either not well seen or not seen at all with white light (Figure 5).

Validation of the targeting ability of the RG-$(gal)_{28}$GSA was confirmed using peritoneally disseminated RFP-transfected SHIN3 xenografts. Spectral fluorescence unmixed images confirmed tumor targeting of RG-$(gal)_{28}$GSA to the same foci as the unmixed RFP spectral images (Figure 6) comparable to previous results confirming both high sensitivity and high selectivity.[24] Specificity to galactose-binding lectins was demonstrated by the decrease in the uptake and fluorescence of RG-$(gal)_{28}$GSA upon co-adminstration of unlabeled $(gal)_{28}$GSA (Figure 7).

Acute Toxicity Studies

Thirty out of 35 mice received an i.p or i.v. injection of either 10x, 20x, 40x, 80x, or 100x standard dose of agent (5 were kept as controls). None of the 35 mice exhibited any signs of toxicity with one exception. A portion of the 80x solution became foamy when drawn into the syringe, and the third mouse of the IV group received some of this foam. Immediately upon injection the mouse exhibited symptoms consistent with micro air emboli: loss of balance, lethargy; but normal behavior returned within 6 hours. Because of her quick recovery and because of the apparent health of the 2 other mice that received the 80x dose, the decision was made to move forward with the 100x i.v. dose. There were no adverse reactions at this dosage. No organ enlargement or damage was noted in any of the mice during post study dissection and examination.

Discussion

A direct amidation approach was used to synthesize the galactosylated human serum albumin wherein galactosamine is directly conjugated to available carboxylic groups of the protein through *in situ* activation using EDC and NHS. The major concern was the potential formation of crosslinked proteins from the reaction of the lysines and *N*-terminus of the protein to the carboxylic groups of another molecule of protein (intermolecular reaction).[25, 26] This intermolecular crosslinking, however, was minimized by using low concentrations of the protein (~1 mg/mL) and the activating agents (~16 mM EDC and ~30 mM galactosamine) and minimal amounts of intermolecularly crosslinked products were observed in gel electrophoresis (see Supplemental Information), and SE-HPLC (see

Supplemental Information). However, we can not discount the formation of intramolecular crosslinking as these would have the same molecular weight as the desired product.

Mass spectral analyses were used to estimate the average number of galactosamine incorporated into the human serum albumin. Human serum albumin has an average molecular weight of ~66 kDa ([M+H] *m/z* 66380.2) containing about 98 combined glutamic and aspartic residues and 59 lysine residues. Although the total number of carboxylic acid residues in HSA is 99 including the *C*-terminus and the total number of amino groups including the *N*-terminus is 60, not all of these are available or accessible for conjugation so we do not expect 99 sugar residues conjugated to HSA.

The mass difference between the galactosylated versus the starting HSA divided by the molecular weight of the sugar residue (galactosamine or glucosamine MW ~ 179) gives us an estimate number of the conjugated sugar. In the direct amidation of galactosamine to HSA, a reaction time of 4 hr at 37°C, gives a mass difference of ~3643 corresponding to 20.4 galactosamine residues per HSA (Figure 1). In comparison, a longer reaction time of 12 hr only increased the galactosamine number to ~ 27.7.

A glucosylated version of the galactosylated HSA, with glucose as an epimer of galactose, was synthesized to compare the sugar selectivity in tumor targeting. A very comparable number of ~28.1 glucosamine residues were conjugated to HSA under the same conditions with a 12 hr reaction time. This seems to suggest that under these conditions (reagent concentration and reaction pH and temperature), the maximum number of sugar molecules that can be incorporated into HSA by direct amidation is ~28.

Blocking the reactive lysines and *N*-terminus through reductive amination with glyceraldehyde followed by amidation reaction with galactosamine (ggHSA), an approach used to synthesize galactosylated bovine serum albumin (Sigma-Aldrich), presumably minimizes the concern for the formation of crosslinked proteins. However, this additional step adds another modification to the protein thus, making analysis and characterization more difficult. It is also more challenging to insure that the same number of modifications in each step occurs.

In vivo fluorescence imaging data confirms binding and tumor uptake for ggHSA which is comparable if not less than the RG-$(gal)_{28}$HSA (see Supplemental Information). This however suggests that there is nothing gained by first blocking the lysine residues with glyceraldehyde before glycosylation. Conversely, the synthesis, characterization, and reproducibility of the final product becomes more complex with additional steps.

The synthesis of the glycosylated HSA emphasizes maximizing the quantity of sugar on the surface of HSA to enable better targeting of and binding to the surface lectins on the tumor cells.[27] Previous studies using avidin as the base protein revealed that it has 4 glucosamine and 5 mannose,[28] galatosylated bovine serum albumin from Sigma-Aldrich contains ~23 galactosamine, and the synthesized galactosylated human serum albumin used in this study contains ~20 galatosamine (RG-$(gal)_{20}$HSA) and ~28 galatosamine (RG-$(gal)_{28}$HSA). In agreement with previous studies,[9, 14] this study demonstrated both *in vitro* and *in vivo* evidence that the fluorescence signal intensities were highest for RG-$(gal)_{28}$HSA versus those optical agents with fewer sugar units.

Sugar specificity was also tested by comparing the selectivity of the ovarian cells lectins to either galactose or glucose. In this study, almost the same number of glucosamine or galactosamine (~28) was conjugated to HSA, however, *in vitro* and *in vivo* data both confirm better binding and higher tumor uptake with the galactose-containing HSA compared to glucose-containing compounds. Specificty of the galactose-binding was further

supported with the in vitro and in vivo blocking studies using co-injection with unlabeled $(gal)_{28}$GSA. Addition of the unlabeled $(gal)_{28}$GSA reduces the log shift and the MFI in the flow cytometry studies using SHIN3 cells (see Supplemental Information) and also decreases the uptake of the RG-$(gal)_{28}$HSA in the in vivo studies using peritoneally disseminated SHIN3 (Figure 7).

Typically, near infrared dyes are chosen for *in vivo* optical imaging because of their superior depth penetration in tissue. However, Rhodamine Green dye was chosen as the fluorophore in this study because they provide sufficient spectral difference from autofluorescence and because once internalized, Rhodamine Green provides the brightest image with a high quantum yield.[11, 14]

Preliminary studies on the toxicity of the Rhodamine Green-$(gal)_{28}$GSA were performed on BALB/c immunocompetent mice as a starting point in the toxicity evaluation of this new agent. Failure of the agent at this point would lead to rethinking of the strategy and looking closely at the toxicity of the dye or of the galactosylated HSA. However, there is reason to be optimistic as the radiolabeled ^{99m}Tc-DTPA galactosylated HSA is well tolerated and is currently used in humans for liver function evaluation,[18, 20-23] but the toxicity of Rhodamine Green dye (also referred to as Rhodamine 110) is not well characterized.

Although RG-$(gal)_{28}$GSA is to be administered intraperitoneally, intravenous administration of the agent was also studied to provide a “worst case scenario” of the entire agent being directly administered systematically. A repeated dosing study was, however, not performed as this agent is most likely to be used only during surgery, which would entail infrequent dosing throughout a patient’s lifetime.

This preliminary toxicity study demonstrates no adverse reactions nor acute toxic effects to the administration of the RG-$(gal)_{28}$GSA agent, when administered intraperitoneally or intravenously even at very high doses of 100x of the standard dose used in the imaging studies. A limitation of this study is that it is performed on only one species, and the validity would be strengthened by a similar result in a non-rodent species but there is no reason to expect different results. A full toxicity evaluation involving at least two species with complete pharmacologic and toxicologic analyses must still be performed for FDA clearance. Still, these results provide a first indication of the safety of RG-$(gal)_{28}$GSA.

Conclusions

Previous studies have used Rhodamine Green conjugated to avidin[15, 29, 30] or to galactosylated bovine serum albumin[14, 24, 29] as a targeted optical agent for ovarian carcinoma. However, these agents are not “clinic” ready, since both avidin[16] and BSA[31-33] are immunogenic. The goal of this study was to synthesize a viable clinically translatable tumor-targeting optical agent such as Rhodamine Green-$(gal)_{28}$GSA to aid in the identification of submillimeter-sized tumor lesions during cytoreductive surgery, thereby leading to a better clinical outcome. We have synthesized a human serum albumin-based tumor targeting optical agent that is believed to be non-immunogenic and has been used extensively in humans in its radiolabeled form.

Two synthetic routes were used to obtain a viable targeting optical agent, however, the small differences in their reactivity suggest that simpler one-step process would be more practical for further translation into a good manufacturing production (GMP) facility. Preliminary toxicity studies on Balb/c mice also demonstrated no toxic or adverse effect with RG-$(gal)_{28}$GSA when administered intraperioneally or intravenously even at 100x of the standard dose used for imaging studies. The study also focused on using Rhodamine Green

dye but other dye conjugates can certainly be tested with very minor changes in the synthesis.

Although we have shown feasibility of this agent, studies using real human tissues would be desirable and complete toxicity studies would also be needed.

Experimental Section

Materials and Instrumentation

Human serum albumin (HSA), β-D-galactosamine, β-D-glucosamine, *N*-(3-dimethylaminopropyl)-*N*'-ethylcarbodiimide hydrochloride (EDC), 2-(N-morpholino)ethanesulfonic acid (MES) monohydrate, MES sodium salt, and sodium acetate were all obtained from Sigma Aldrich (St. Louis, MO) and used as supplied. Glacial acetic acid was obtained from Mallinckrodt (Phillipsburg, NJ). *N*-hydroxysuccinimidyl ester of Rhodamine Green 5(6)-CR 110 SE mixed isomers were obtained from Invitrogen (Carlsbad, CA).

Instrumentation

Size exclusion HPLC (SE-HPLC) was performed using a Beckman System Gold (Fullerton, CA) equipped with Model 126 solvent delivery module, a Model 168 UV detector (λ 254 and 280 nm), and a JASCO fluorescence detector (excitation 502 nm and emission at 532 nm) controlled by 32 Karat software. Size exclusion chromatography was performed on a Superose™ 12 10/300GL column (GE Amersham, Pittsburg, PA) and/or TSKgel G2000SWxl (Tosoh Bioscience LLC, Montgomeryville, PA) eluted for 45 min using phosphate buffered saline (1X PBS) solution at 0.5 mL/min.

Matrix-assisted laser desorption-time of flight mass spectrometry (MALDI-TOF MS) data was acquired on an AXIMA Performance (Shimazdu, Manchester, U.K.) using linear positive ionization mode equipped with a 337 nm nitrogen laser operating at 50 Hz. Samples were analyzed at a concentration of 20 fmol/μL and were prepared using purified sinapinic Acid (20 mg/mL in 50% acetonitrile with 0.1% trifluoroacetic acid in water) (Laser BioLabs, Sophia-Antipolis, France). Spotting was performed using the dried droplet method using 0.5 μL sample and 0.5 μL matrix.

Direct Amidation of HSA with galactosamine (GSA)

Human serum albumin (300 mg) was dissolved in 300 mL of 0.5 M MES solution at pH 5.25. Galactosamine (1.62 g) and EDC (0.92 g) were then added in sequence to the HSA solution and was then placed in a shaking water bath at 37°C for 12 hr ($(gal)_{28}$GSA) and 4 hr ($(gal)_{20}$GSA). The reaction mixture was then quenched with 50 mL 1.0 M sodium acetate pH ~4.5 and dialyzed exhaustively against 10 mM sodium acetate pH ~7 using a Tangential Flow Filtration system (Millipore, Billerica, MA) equipped with a Pellicon XL 50 cm^2 Biomax 30 cassette (MWCO 30,000; Millipore) and concentrated down to ~17 mL. Total protein concentration for this intermediate galactosylated human serum albumin (GSA) was then determined using the Lowry method (225.94 mg, 75.3% yield). MALDI-TOF MS: starting HSA: *m/z* 66380.2; $(gal)_{28}$GSA *m/z* 71332.2; $(gal)_{20}$GSA *m/z* 70023.0

For "*endotoxin-free*" synthesis, all containers and buffers were sterile and pyrogen-free, the reaction and dialysis were kept sterile, and the product solution was sterile-filtered after dialysis.

Direct Amidation of HSA with glucosamine

High glucose-containing HSA ($(glu)_{28}$GSA) was analogously prepared using the same procedure as above, shaking the reaction mixture for 12 hr at 37°C. Total protein concentration was determined by the Lowry method (259.5 mg, 86.5% yield). MALDI-TOF MS $(glu)_{28}$GSA *m/z* 71408.4

Rhodamine Green conjugation to GSA

For a small scale synthesis, 400 μg of the *glycosylated* GSA was incubated with *N*-hydroxysuccinimidyl ester of Rhodamine Green (24 nmol) in 0.1 M Na_2HPO_4 (200 μL, pH 8.4) for 30 min at room temperature. The mixture was then purified using a PD-10 column (GE Healthcare, Milwaukee, WI, USA) eluted with 1x PBS.

To a 12 mL solution of *glycosylated* serum albumin (GSA) (159 mg) in 10 mM sodium acetate, 5 mL 0.1 M sodium phosphate at pH ~8 was added. *N*-hydroxysuccinimidyl ester of Rhodamine Green was then added to the glycosylated GSA solution and allowed to react for 3 hr at room temperature. The reaction mixture was then exhaustively dialyzed against 10 mM sodium acetate pH ~7 using the Tangential Flow Filtration system equipped with a Pellicon XL 50 cm^2 Biomax 30 cassette and concentrated down to 10 mL. Total protein concentration for the final product was determined using the Lowry method (87.9 mg, 55% yield from GSA) and the dye concentration was determined spectrophotometrically (~6.2 dye molecule per GSA on average, λ 504 nm, ε 78, 000 cm^{-1}).

Endotoxin Assay

A gel-clot Limulus Amebocyte Lysate (LAL) assay was used to detect and measure the level of endotoxin in the final product. A LAL kit (Charles River Laboratories International, Wilmington, MA) with 0.125 EU/mL sensitivity was used to test for endotoxin level in the final product and the endotoxin level at each IP dose used in the acute toxicity studies was also determined. Assays were performed in triplicates according to the manufacturer's instruction with sterile saline solution as negative control and positive water (endotoxin) controls that was also provided in the kit.

Cell Culture

Human ovarian adenocarcinoma cell line SHIN3 (provided by Dr. S. Imai, Nara, Japan)[34] and RFP-transfected DSRed2 SHIN3 (from Dr. Y. Hama[24]), was grown in RPMI-1640 medium (BioWhittaker) containing 10% FBS, 0.03% L-glutamine, 100 U/mL penicillin and 100 μg/mL streptomycin at 37°C in 5% CO_2. Epidermoid carcinoma cell line A-431 (ATCC) and human colorectal adenocarcinoma LS 174T (ATCC) were grown in DMEM (BioWhittaker) containing 10% FBS and 10% non-essential amino acid (NEAA) at 37°C in 5% CO_2. Mammary epithelial adenocarcinoma MCF7 (ATCC), human pancreatic carcinoma SHAW (ATCC), human ovarian adenocarcinoma NIH:OVCAR-3 (ATCC) and OVG-1 (a gift from from Dr. J. Mitchell, NCI, NIH), and human prostatic adenocarcinoma PC-3 (ATCC) were grown in RPMI 1640 containing 10% FBS and 10% non-essential amino acid (NEAA) at 37°C in 5% CO_2. Human ovarian adenocarcinoma SK-OV-3 (ATCC) was grown in McCoy's 5A media (Biowhittaker) containing 10% FBS and 10% non-essential amino acid (NEAA) at 37°C in 5% CO_2.

Fluorescence Microscopy Studies

SHIN3 cells were plated on a cover glass–bottomed culture well and incubated for 16 hr. Then Rhodamine Green-glycosylated human serum albumin was added to the medium (3 μg/mL), and the cells were incubated for 6 hr. Cells were washed once with PBS, and fluorescence microscopy was performed using an Olympus BX61 microscope (Olympus

America, Inc., Melville, NY) equipped with the following filters: excitation wavelength, 530 to 570 nm, and emission wavelength 590 nm long pass. Transmitted light differential interference contrast images were also acquired

One-Color Flow Cytometry Studies

Cells were placed on a 12-chamber well and incubated for 24 hr. The Rhodamine Green-glycosylated HSA conjugates (3 μg/mL) were added to the medium and incubated for 6 hr at 37°C in 5% CO_2. For blocking study, 100 μg/mL of the unlabeled $(gal)_{28}$HSA (no dye conjugate) was added at the same time as RG-$(gal)_{28}$HSA. After incubation, the cells were washed with cold 1x PBS and flow cytometry was performed employing 488 nm laser for excitation. Signals from cells were collected using 530/30 nm band-pass filter. Cells were analyzed in a FACScan cytometer (BD Bioscience, San Jose, CA) and data were analyzed using CellQuest software (BD). The fluorescence intensity was expressed as mean fluorescence intensity (MFI).

In vivo Studies

All procedures were performed in accordance with the National Institutes of Health guidelines on the use of animals in research and were approved by the Animal Care and Use Committee of the National Cancer Institute.

Animal Tumor Model

SHIN3 cells (2×10^6) suspended in 300 μL of 1x PBS were injected intraperitoneally into female athymic nu/nu mice (National Cancer Institute Animal Production Facility, Frederick, MD) and experiments with peritoneally disseminated xenografts were carried out approximately 3 weeks after cell injection.

In Vivo Fluorescence Imaging

Tumor-bearing mice received an i.p. injection of 20 μg of Rhodamine Green HSA conjugates diluted in 300 μL of 1x PBS. For blocking study, 10 mg of unnlabeled $(gal)_{28}$HSA (no dye conjugate) was coinjected with RG-$(gal)_{28}$HSA. The mice were then euthanized by CO_2 inhalation 4 hr after agent administration. The abdominal wall is excised and white-light photos and spectral fluorescence images of the entire exposed abdomen and a loop of the bowel with mesentery from each mouse was obtained using a Maestro In Vivo Imaging System (CRi, Woburn, MA). A band-pass filter from 445 to 495 nm and a long pass filter over 515 nm were used for excitation and emission, respectively. The tunable filter was automatically stepped in 10-nm increments from 500 to 800 nm while the camera captured images each wavelength interval with constant exposure. Commercially available Maestro software (Nuance Version 2p23 CRi) equipped with spectral unmixing algorithms was used to create the spectral fluorescence composite images.

A direct comparison of the fluorescence intensity of the different Rhodamine Green conjugated to glycosylated-GSA and a control Rhodamine Green-HSA treated xenografts were made by imaging the tumor nodules side-by-side *ex vivo*.

Acute Dose Toxicity

All toxicity testing were performed with “endotoxin-free” RG-$(gal)_{28}$GSA. To determine the minimum dose of acute toxicity, we administered 10 mg/kg (10x) to 2 groups of 3 mice. One group received their injections intravenously (IV), the other, intraperitoneally (IP). As ovarian cancer is gender specific, we used only female Balb/c immunocompetent mice, between 6-8 weeks old. All IV doses were administered in volumes of 200 μl, and IP doses were administered in volumes of 300 μl. The mice were then closely observed for signs of

toxicity by an experienced animal handler at regular intervals over 7 days. Signs and symptoms of toxic effects include rashes, hair loss, and discoloration as well as common sickness behaviors (including anorexia, reduced grooming, excessive sleep, and/or reduced social contact).[35] If the mice survived seven days, they were euthanized and a necropsy was performed to look for signs of organ enlargement or damage. Barring any signs of toxicity or necropsy findings, the study was repeated with an escalated dose of 20 mg/kg (20x), and proceeded in this manner with doses of 40 mg/kg (40x), 80 mg/kg (80x), and 100 mg/kg (100x). If at any point signs of toxicity were observed, the mice were euthanized, and no further studies of higher doses were performed with that injection method.

Supplementary Material

Refer to Web version on PubMed Central for supplementary material.

Acknowledgments

This research was supported by the Intramural Research Program of the NIH, National Cancer Institute, Center for Cancer Research.

Abbreviations

HSA	human serum albumin
GSA	galactosylated human serum albumin
RG	Rhodamine Green dye
RG-(gal)$_x$GSA	Rhodamine Green conjugated to galactosylate human serum albumin with *x* denoting average number of galactosamine units
RG-(glu)$_x$GSA	Rhodamine Green conjugated to glucosylated human serum albumin with *x* denoting average number of glucosamine units
RG-HSA	Rhodamine Green conjugated to human serum albumin

References

1. Heron MP, Hoyert DL, Xu J, Scott C, Tejada-Vera B. Deaths: Preliminary data for 2006. National Vital Statistics Reports. 2008; 56:1–52. [PubMed: 18092547]
2. Jemal A, Siegel R, Ward E, Hao Y, Xu J, Murray T, Thun MJ. Cancer statistics, 2008. CA Cancer J Clin. 2008; 58:71–96. [PubMed: 18287387]
3. Hoffman RM. The multiple uses of fluorescent proteins to visualize cancer in vivo. Nat Rev Cancer. 2005; 5:796–806. [PubMed: 16195751]
4. Hoffman RM, Yang M. Subcellular imaging in the live mouse. Nat Protocols. 2006; 1:775–782.
5. Hoffman RM, Yang M. Color-coded fluorescence imaging of tumor-host interactions. Nat Protocols. 2006; 1:9–928.
6. Hoffman RM, Yang M. Whole-body imaging with fluorescent proteins. Nat Protocols. 2006; 1:1429–1438.
7. Kishimoto H, Zhao M, Hayashi K, Urata Y, Tnaka N, Fujiwara T, Penman S, Hoffman RM. In vivo internal tumor illumintation by telomerase-dependent adenoviral GFP for precise surgical navigation. Proc. Natl. Acad. Sci. USA. 2009; 106:14515–14517.
8. Gunn AJ, Brechbiel MW, Choyke PL. The emerging role of molecular imaging and targeted therapeutics in peritoneal carcinomatosis. Expert Opin Drug Deliv. 2007; 4:389–402. [PubMed: 17683252]

9. Gunn AJ, Hama Y, Koyama Y, Kohn EC, Choyke PL, Kobayashi H. Targeted optical fluorescence imaging of human ovarian adenocarcinoma using a galactosyl serum albumin-conjugated fluorophore. Cancer Sci. dnlm. 2007; 98:1727–1733.
10. Stockert RJ. The asialoglycoprotein receptor: relationships between structure, function, and expression. Physiol. Rev. 1995; 75:591–609. [PubMed: 7624395]
11. Hama Y, Urano Y, Koyama Y, Bernardo M, Choyke PL, Kobayashi H. A comparison of the emission efficiency of four common green fluorescence dyes after internalization into cancer cells. Bioconjugate Chem. 2006; 17:1426–1431.
12. Hama Y, Urano Y, Koyama Y, Kamiya M, Bernardo M, Paik R, Krishna MC, Choyke PL, Kobayashi H. In vivo spectral fluorescence imaging of submillimeter peritoneal cancer implants using a lectin-targeted optical agent. Neoplasia. 2006; 8:607–612. [PubMed: 16867223]
13. Hama Y, Urano Y, Koyama Y, Choyke PL, Kobayashi H. Targeted optical imaging of cancer cells using lectin-binding BODIPY conjugated avidin. Biochem. Biophys. Res. Commun. 2006; 348:807–813. [PubMed: 16904640]
14. Hama Y, Urano Y, Koyama Y, Choyke PL, Kobayashi H. D-galactose receptor-targeted in vivo spectral fluorescence imaging of peritoneal metastasis using galactosamin-conjugated serum albumin-rhodamine green. J Biomed Optics. 2007; 12:051501-1–051501-9.
15. Hama Y, Urano Y, Koyama Y, Choyke PL, Kobayashi H. Targeted optical imaging of cancer cells using lectin-binding BODIPY conjugated avidin. Biochem. Biophys. Res. Commun. 2006; 348:807–813. [PubMed: 16904640]
16. Scott D, Nitecki DE, Kindler H, Goodman JW. Immunogenicity of biotinylated hapten-avidin complexes. Mol. Immunol. 1984; 21:1055–1060. [PubMed: 6440008]
17. Stadalnik RC, Vera DR, Woodle ES, Trudeau WL, Porter BA, Ward RE, Krohn KA, O'Grady LF. Technetium-99m NGA functional hepatic imaging: preliminary clinical experience. J Nucl Med. 1985; 26:1233–1242. [PubMed: 2997417]
18. Ikuyo E, Kenjiro O, Atsushi F, Akira N, Shiro M. Tc-99m GSA scintigraphy for evaluation of liver function. Correlations with histological grading and staging (new Inuyama classification). Jpn J Med Imaging. 2000; 19:259–267.
19. Kim E-M, Jeong H-J, Park I-K, Cho C-S, Kim C-G, Bom H-S. Hepatocyte-targeted nuclear imaging using 99mTc-galactosylated chitosan: conjugation, targeting, and biodistribution. J Nucl Med. 2005; 46:141–145. [PubMed: 15632044]
20. Suzuki Y, Kohno Y, Takeda Y, Hiraki Y. Evaluation of liver function parameters by Tc-99m-GSA using multivariate nalysis: a study of 47 clinical cases. Acta Med Okayama. 1999; 53:225–232. [PubMed: 10561731]
21. Mitsumori A, Nagaya I, Kimoto S, Akaki S, Togami I, Takeda Y, Joja I, Hiraki Y. Preoperative evaluation of hepatic functional reserve following hepatectomy by technetium-99m galatosyl human serum albumin liver scintigraphy and computed tomography. Eur J Nucl Med. 1998; 25:1377–1382. [PubMed: 9818276]
22. Schneider PD. Preoperative assessment of liver function. Surg Clin N Am. 2004; 84:355–373. [PubMed: 15062650]
23. Hama Y, Kosuda S, Iwasaki Y, Kaji T, Kusano S. Technetium Tc 99m DTPA galactosyl human serum albumin to measure in hepatic functional reserve after transcatheter arterial emabolization of the liver. Can Assoc Radiol J. 2001; 52:399–403. [PubMed: 11780551]
24. Hama Y, Urano Y, Koyama Y, Gunn AJ, Choyke PL, Kobayashi H. A self-quenched galactosamine-serum albumin-rhodamine X conjugate: a "smart" fluorescent molecular imaging probe synthesized with clincally applicable material for detecting peritoneal ovarian cancer metastases. Clin. Cancer Res. 2007; 13:6335–6343. [PubMed: 17975145]
25. Valuev IL, Chupov VV, Valuev LI. Chemical modification of polymers with physiologically active species using water-soluble carbodiimides. Biomaterials. 1998; 19:41–43. [PubMed: 9678848]
26. Pieper JS, Hafmans T, Veerkamp JH, van Kuppevelt TH. Development of tailor-made collagen-glycosaminoglycan matrices: EDC/NHS crosslinking and ultrastructural aspects. Biomaterials. 2000; 21:581–593. [PubMed: 10701459]

27. Kitov PI, Bundle DR. On the nature of multivalency effect: a thermodynamic model. J. Am. Chem. Soc. 2003; 125:16271–16284. [PubMed: 14692768]
28. Huang T-S, DeLange RJ. Egg white avidin. II. Isolation, composition, and amino acid sequences of the tryptic peptides. J Biol Chem. 1971; 246:686–697. [PubMed: 5100762]
29. Hama Y, Urano Y, Koyama Y, Kamiya M, Bernardo M, Paik RS, Krishna MC, Choyke PL, Kobayashi H. In vivo spectral fluorescence imaging of submillimeter peritoneal cancer implants using a lectin-targeted optical agent. Neoplasia. 2006; 8:607–612. [PubMed: 16867223]
30. Hama Y, Urano Y, Koyama Y, Choyke PL, Kobayashi H. Activatable fluorescent molecular imaging of peritoneal metastases following pretargeting with a biotinylated monoclonal antibody. Cancer Res. 2007; 67:3809–3817. [PubMed: 17440095]
31. Stark JM, Spitznagel JK. Immunogenecity of bovine serum albumin and its oligopolymers in CBA mice. J Immunol. 1972; 108:800–806. [PubMed: 5011757]
32. Wainer BH, Fitch FW, Rothberg RM, Fried J. Morphine-3-succinyl-bovine serum albumin: an immunogenic hapten-protein conjugate. Science. 1972; 176:1143–1145. [PubMed: 5064326]
33. Heddleson RA, Allen JC. Relative immunogenecity of betal-lactoglobulin, bovine serum albumin, and model acid whey product. Nutr Res. 1997; 17:505–514.
34. Imai S, Kiyozuka Y, Maeda H, Noda T, Hosick HL. Establishment and characterization of a human ovarian serous adenocarcinoma cell line that produces the tumor markers CA-125 and tissue polypeptide antigen. Oncology. 1990; 47:177–184. [PubMed: 2314830]
35. Kent S, Bluthe R-M, Kelley KW, Dantzer R. Sickness behavior as a new target for drug development. Trends Pharmacol. Sci. 1992; 13:24–28. [PubMed: 1542935]

Briefs

A non-toxic targeted optical agent Rhodamine green-galactosylated human serum albumin is synthesized in two simple steps and can be used to improve intraoperative and/or endoscopic tumor detection and resection.

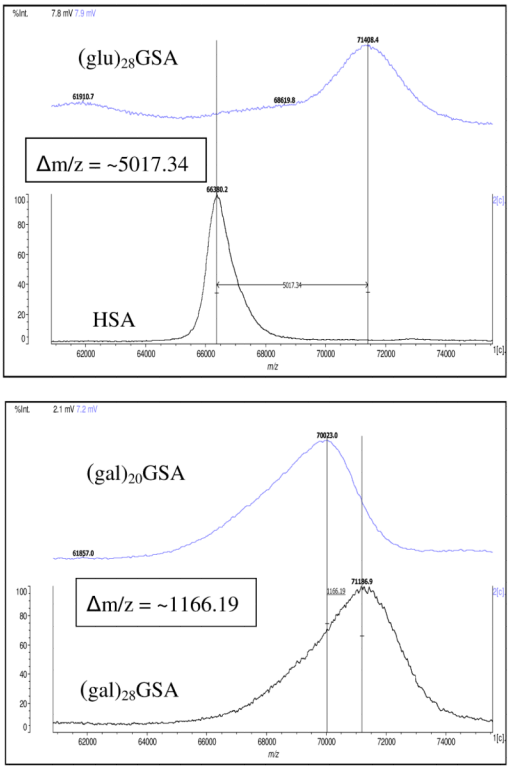

Figure 1.

Mass spectral data showing the difference in *m/z* of 5017.34 from the starting material human serum albumin (HSA) to the glucosylated GSA ($(glu)_{28}GSA$) (top portion) indicating a modification of ~28 glucosamine to HSA. Lower portion demonstrates the Δ *m/z* of 1166.19 between the galactosylated GSA's at different reaction time estimating the difference in the number of galactosamine to ~8.

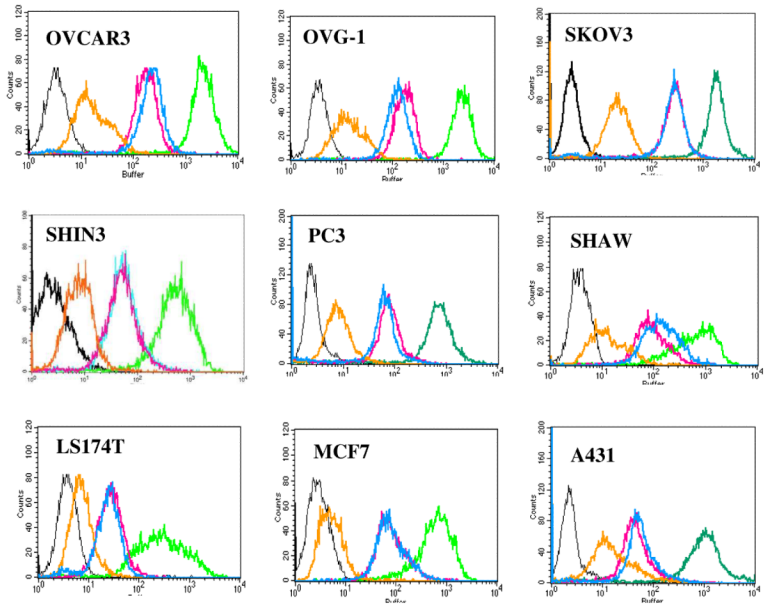

Figure 2.

Flow cytometry studies from different human adenocarcinoma cell lines after incubation with 3 μg/mL of RG-$(gal)_{28}$GSA (green), RG-$(gal)_{20}$GSA (blue), RG-$(glu)_{28}$GSA (pink), RG-HSA (orange), and buffer (black). The percentage fluorescently-gated cells and mean fluorescence intensity is highest with RG-$(gal)_{28}$GSA incubation for all cell lines tested.

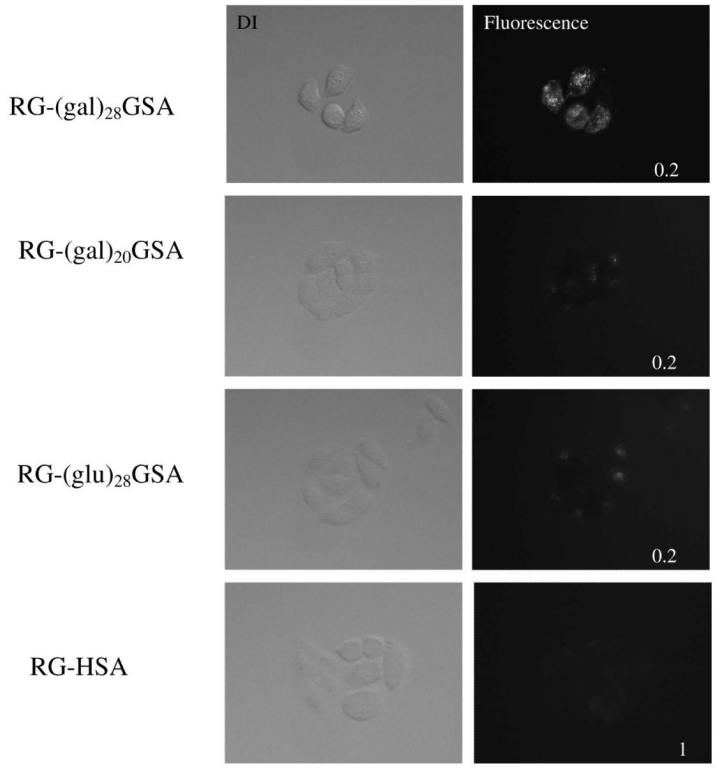

Figure 3.
Fluorescence microscopy images (right panel) and differential interference contrast imaging (left panel) of SHIN3 cells 6 hr after incubation with 3 μg/mL of the Rhodamine dye conjugates of the glycosylated GSA and non-glycosylated HSA. Cells incubated with the glycosylated GSA demonstrated internalization of the agent with the $(gal)_{28}$GSA showing the largest number of fluorescent dots within the cytoplasm under the same exposure time (200 ms) and with RG-HSA showing no fluorescence within the SHIN3 cells even at longer exposure time (1 s).

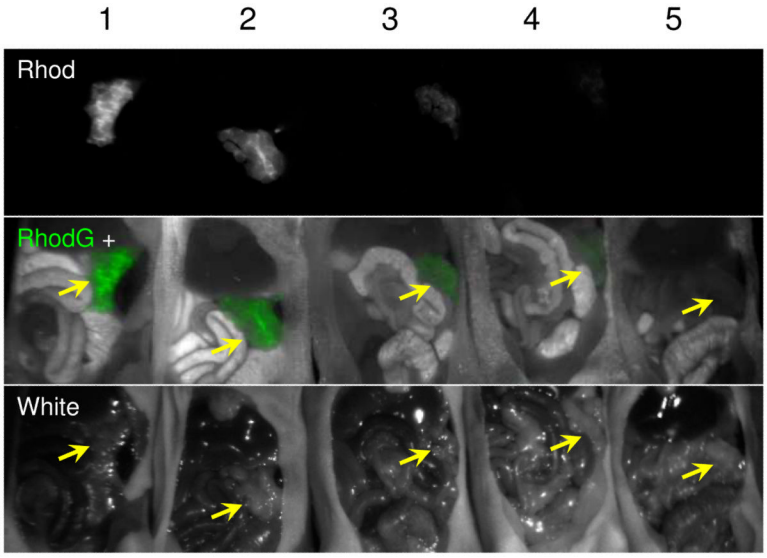

Figure 4.

Spectral fluorescence imaging of the peritoneal cavities of SHIN3-xenografted mice 4 hr after intraperitoneal injection of 20 μg of the **1**:RG-$(gal)_{28}$GSA, **2**:RG-$(gal)_{20}$GSA, **3**:RG-$(glu)_{28}$GSA, **4**:RG-HSA, and a **5**:nontreated mouse. Spectral unmixed Rhodamine Green fluorescence images (upper), composite (with autofluorescence) (middle) images, and white light images (lower) are shown. Aggregated large tumor foci are pointed by the arrows.

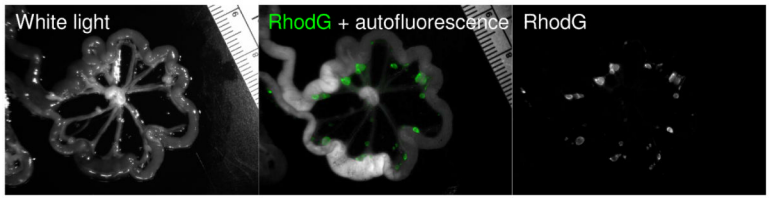

Figure 5.
Small SHIN3 implants are detected using RG-$(gal)_{28}$GSA on the peritoneal membranes as shown by the spectral fluorescence images with the spectral unmixed Rhodamine green fluorescence (right most panel), composite (with autofluorescence) (middle panel), and white light (left most panel) images.

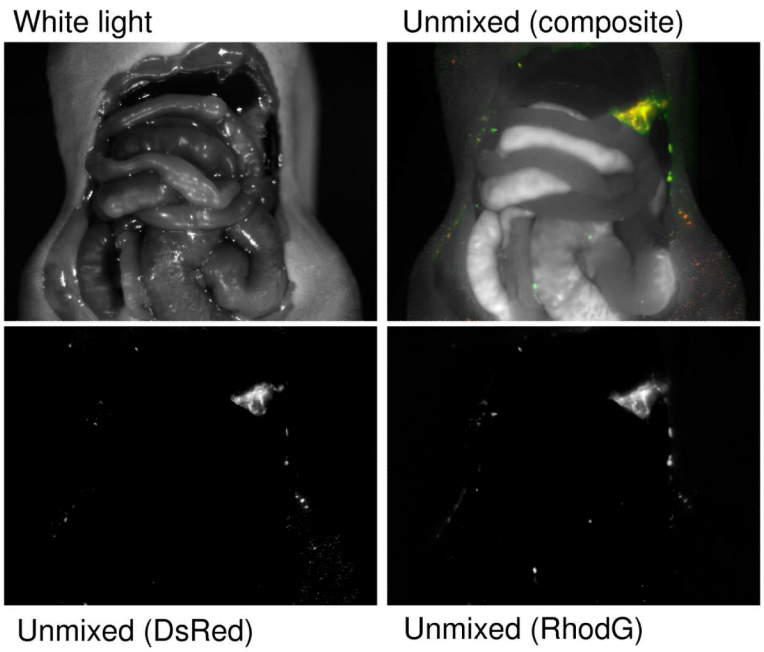

Figure 6.

Sensitivity and specificity of the RG-$(gal)_{28}$GSA was validated using RFP-transfected SHIN3 ovarian cancer-bearing mice. The spectral fluorescence images were unmixed based on the spectral patterns of Rhodamine Green (lower right panel), RFP (DsRed) (lower left panel), and autofluorescence.

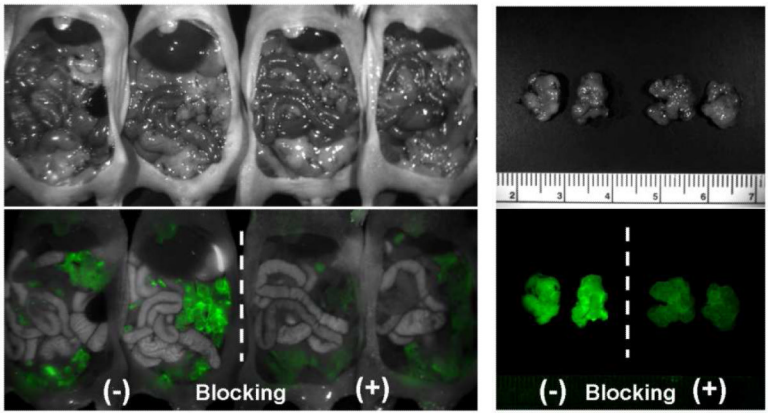

Figure 7.

Receptor-mediated uptake was demonstrated by the decrease in the uptake of RG-$(gal)_{28}$GSA upon co-adminstration of 10 mg of unlabeled $(gal)_{28}$GSA with 20 μg of RG-$(gal)_{28}$GSA.